

Lambertian nature of tissue phantoms for use as calibrators in near infrared fluorescence imaging

Maritoni Litorja*^a, Simón Lorenzo^b, Banghe Zhu^c and Eva Sevick Muraca^c

^aNational Institute of Standards and Technology, Gaithersburg, MD 20899

^bDept. of Physics and Astronomy, Louisiana State University, Baton Rouge, LA 70803

^cBrown Foundation Institute for Molecular Medicine,
Univ. of Texas Houston Health Science Center, Houston, TX 77030

ABSTRACT

The use of tissue phantoms as calibrators to transfer SI-referenced scale to an imager offers convenience, compared to other methods of calibration. The tissue phantoms are calibrated separately for radiance at emission wavelength per irradiance at excitation wavelength. This calibration is only performed at a single geometric configuration, typically with the detector normal to the sample. In the clinic however, the imager can be moved around, resulting in a geometric configuration different from the calibration configuration. In this study, radiometric measurements are made at different sample-imager angles to test whether the tissue phantoms are Lambertian and the angular limits to which the calibration values hold true.

Keywords: near infrared fluorescence imaging, molecular imaging, radiometry, calibration, tissue phantoms

1. INTRODUCTION

The acquired light signal in *in vivo* fluorescence imaging is intended to correlate to the presence, or if possible, quantity of a desired biological marker. Inside the tissue, the fluorescence emission is dependent on factors of biological (e.g., binding to desired marker), chemical (e.g. proticity, solvation, competitive energetic pathways), and physical (attenuation of excitation and emission radiation, scattering) origin. Once the emitted fluorescence exits the patient (e.g skin) surface into free space and of which a portion is collected by the imager situated at some distance away from the patient, it is a physical measurement of light involving primarily geometric optics. The measurement sources of uncertainty are the same as that of other measurements of a light source.

The imager is a light collector and its performance can be specified using light, independent of the molecular probe. Spectrally, the performance specification needs to be relevant to the molecular probe the imager is intended for use.

1.1 Radiometric Calibration

In order to quantify the amount of fluorescence emitted from the surface (patient), the imager's quantitative response to light (responsivity) has to be calibrated. Calibration is the process where the instrument acquires a scale by virtue of comparisons against a standard. It is an important task in the validation of diagnostic and therapeutic devices. It provides the daily user with confidence in the performance of the device to the specified task.

A photodetector such as the fluorescence imager can be calibrated to acquire a responsivity scale. That is, the imager's signal in digital counts can be correlated to the amount of light detected in units traceable to the International System (SI). Being traceable to the SI is highly advantageous because the SI is anchored in physical laws and maintained by an international system of laboratories which underpins the global scientific and commercial measurements. The fluorescence imager can be calibrated against a standard detector, a standard source, or through the use of a reference material.[1]

1.2 Radiometric Units

There are various units by which the quantity of light can be expressed. The choice of radiometric quantity and therefore units to use in a measurement is fit-for-purpose. For example, radiant flux (power) with units of watts (W or Js⁻¹) is an appropriate quantity only if the light to measure underfills the detector, such as in the case of measuring the power in a laser beam. Radiance with units of W m⁻² sr⁻¹ is typically a quantity associated with real light sources. Irradiance with

units of $W m^{-2}$ is the appropriate unit to measure how much light is incident on a given surface area. Fig. 1 illustrates the difference between radiance L and irradiance E .

Tissue phantoms consisting of quantum dots dispersed with titanium dioxide to mimic tissue optical scatterers in a polyurethane matrix have been shown to be robust enough to serve as near infrared fluorescence imager calibrators.[2] It is a good candidate as a reference material to use as transfer or working standard to carry SI-traceable scale for light measurements. Currently there are no transfer standard reference materials for use in the near infrared with radiometric units.

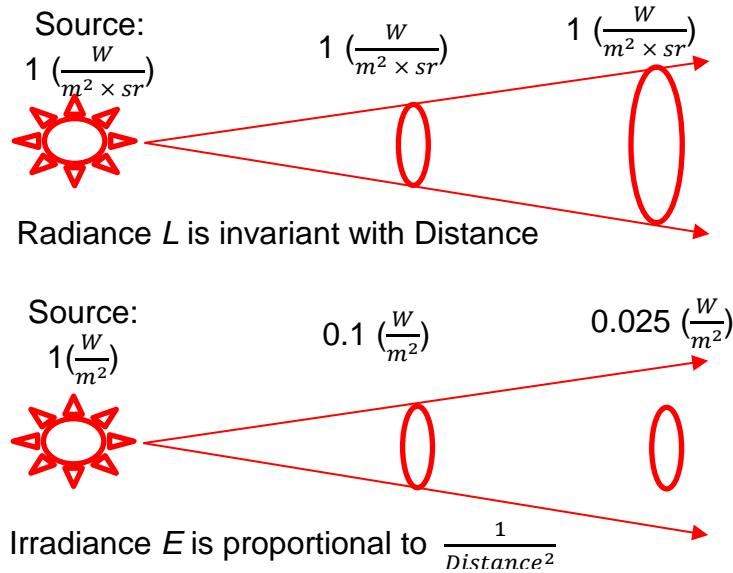


Figure 1. Illustration on the differences between radiance and irradiance variation with distance from source.

The spectral radiance $L_{\lambda em}$ ($W m^{-2} sr^{-1}$) _{λem} from the fluorescence emission of the tissue phantom is a function of the spectral irradiance of the excitation radiation $E_{\lambda ex}$ ($W m^{-2}$) _{λex} and the fluorescence characteristics $F_{\lambda em, \lambda ex}$ of the material

$$L_{\lambda em} = F_{\lambda em, \lambda ex} \cdot E_{\lambda ex} \quad (1)$$

Here we use the special character F as an aggregate fluorescence yield factor for radiometry purposes, to distinguish it from the normally reported molar fluorescence yield of the pure fluorophore, which is an intrinsic optical property of the material. The factor $F_{\lambda em, \lambda ex}$ to be determined in a separate calibration procedure, will need to have units of spectral radiance at emission wavelength per spectral irradiance at excitation wavelength ($W m^{-2} sr^{-1}$) _{λem} / ($W m^{-2}$) _{λex} . With the calibrated tissue phantom and the irradiance of the excitation radiation $E_{\lambda ex}$ measured at the time of image collection, the spectral radiance emitted $L_{\lambda em}$ by the phantom can be known. Since the phantoms then act as light sources of known radiance, and the collection geometry are known (m^2 and sr), the signal counts correlated to that radiance can then be converted to watts (W). We have recently shown the procedure of transferring the calibration scale from a photodiode, to a laser input into an integrating sphere matching radiance of the tissue phantoms.[3] Since this procedure is not readily accessible to most laboratories, a convenient method is to have the tissue phantoms calibrated using a dedicated measurement station, using the choice of excitation and emission wavelengths for which the clinical imager will be used.

1.3 Angular distribution of emission

The optical properties of the tissue phantoms as radiator (fluorescence emission) needs to be studied as a matter of course for materials intended for use as reference standards. Ideal extended sources are assumed to be Lambertian, diffusely radiating in all directions. That is, the radiance measured at all angles with respect to the surface normal is constant; and that the irradiance measured at the observation plane follows Lambert's cosine law.[4] In reality, extended sources are not perfectly Lambertian or the angular range with respect to surface normal at which the radiance is constant is limited.

2. LABORATORY MEASUREMENTS

2.1 Measurements of Radiance

The tissue phantom is a photoactivated light source, as opposed to an electrically driven light bulb, a common calibrator for radiometry. Since the tissue phantoms are intended to be used as radiance calibrators, we examine its properties as a radiator. The objective of the measurement is to compare the tissue phantom radiance with respect to distance to that of a typical lamp calibrator. Figure 2 illustrates the measurement setup in the laboratory for measuring radiance. The radiance from one tissue phantom is compared to that of a typical tungsten halogen lamp. The detector used to measure radiance is a NIST-calibrated silicon photodiode. The excitation radiation for the tissue phantom is supplied by a 785 nm laser, with the beam expanded using a Galilean telescope assembly such that the laser uniformly illuminated the whole surface of the tissue phantom. A field stop is placed in front of the tissue phantom to define the source area. An 830 nm bandpass filters is placed in the detection optical path to limit the band fraction detected. All optical components are placed on an optical rail. The detector assembly is placed at least 300 mm away from the source. The radiance is then measured at different source-detector distances. Baffles and shields comprising of black cloth, and black painted metal shields are used. The photodiode assembly includes a series of baffles to minimize stray light. An aperture is placed in front of the photodiode to define the collection area. The tissue phantom is replaced by a tungsten halogen calibrated lamp source and its radiance measured. Results from the variation of radiance with distance for the tungsten halogen lamp calibrator and the tissue phantom are shown in Figure 3. While the radiance level of the tissue phantom is

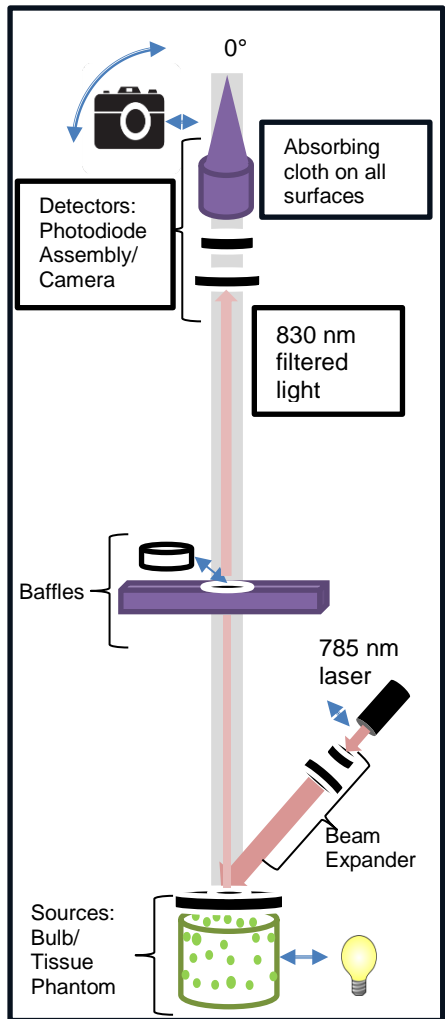


Figure 2. Illustration of the laboratory measurement setup for radiance. Distances are not drawn to scale.

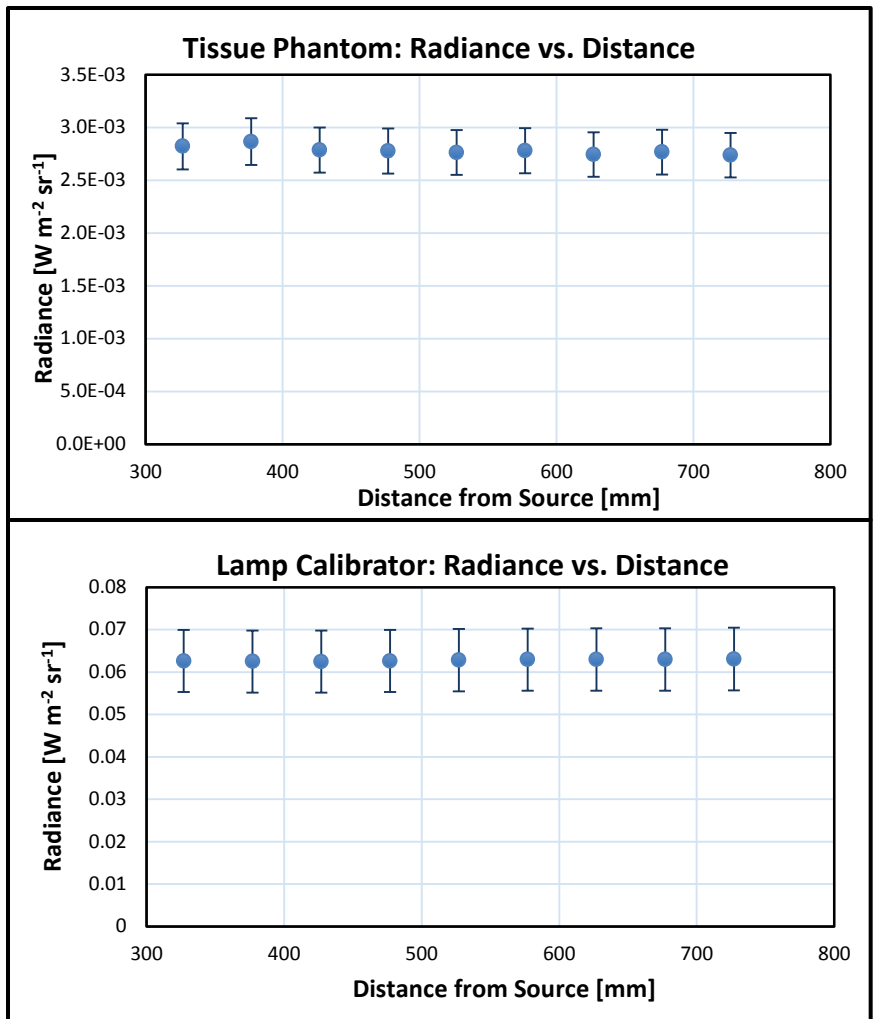


Figure 3. Radiance of tissue phantom (top) is constant with distance, similar to a source calibrator (bottom).

much lower than a lamp calibrator, the value is constant with distance, as is desired in a calibrator. The radiance values have an estimated 1 % relative uncertainty at coverage factor of $k=1$. The steps in estimating the standard uncertainty in radiance is discussed in Sec. 2.2.

It should be noted that a tungsten halogen lamp with its broadband spectral output is not an appropriate light source to calibrate the imager, even with a bandpass filter since the detector is sensitive over the entire visual range and the filter has a non-zero throughput outside of the specified 10 nm bandpass. The lamp introduces stray light into the camera. Moreover, unlike the tissue phantom, its radiance does not have any relationship to the 785 nm excitation radiation. In calibration terms, it is dissimilar to the radiance source being interrogated by the imager for its intended use.

2.2 Uncertainty in Radiance Measurements

The photocurrent generated at the photodiode by the collected light is converted to voltage, amplified and measured using a multimeter. The total radiance collected giving rise to this signal is

$$L_\lambda = \frac{v}{s_{\phi,\lambda} \cdot \Delta_\lambda \cdot G \cdot \Gamma} \quad (2)$$

where L_λ is the spectral radiance of the source with units of $\text{W m}^{-2} \text{sr}^{-1} \text{nm}^{-1}$

v is the voltage measured with units of V

$s_{\phi,\lambda}$ is the spectral flux (power) responsivity of the detector with units of $\text{A W}^{-1} \text{nm}^{-1}$

Δ_λ is the bandwidth of the filter with units of nm

G is the amplifier gain setting with units of V A^{-1}

Γ is the throughput of the optical configuration, defined in this optical configuration as

$$\Gamma = A_d \cdot \omega_s \cdot T \quad (3)$$

A_d is the receiving area of the detector with units of m^2

ω_s is the solid angle of the source viewed by the detector with units of steradian (sr) and approximated as

$$\omega_s = \frac{A_s}{d^2}. \quad A_s \text{ is the area of the source and } d \text{ the distance between the source and detector at the optic axis (centers of source and detector planes). Note that } \omega_d = \frac{A_d}{d^2} \text{ since radiance is invariant with distance.}$$

T is the filter transmittance

To estimate the combined uncertainty $u_c^2(L_{830})$ in radiance value L_{830} computed from the measured voltage signal from the tissue phantom as measured by the photodiode with a filter, we follow the method of propagation of uncertainties [5] in Equation (4) or its relative form (Equation (5)) for the radiance measurement equation in Equation (2) and Equation (3).

$$u_c^2(L_\lambda) = \sum_{i=1}^m c_i^2 u^2(x_i) + 2 \sum_{i=1}^{m-1} \sum_{j=i+1}^m c_i c_j u(x_i, x_j) \quad (4)$$

$$u_c^2(L_\lambda) = L_\lambda^2 \cdot \left[\sum_{i=1}^m \left(c_{i,r} \cdot \frac{u(x_i)}{x_i} \right)^2 + 2 \sum_{i=1}^{m-1} \sum_{j=i+1}^m c_{i,r} c_{j,r} \frac{u(x_i, x_j)}{x_i x_j} \right] \quad (5)$$

$c_i = \frac{\partial L_\lambda}{\partial x_i}$ is the absolute sensitivity coefficient and $c_{i,r}$ the relative sensitivity coefficient to each variable

x_i = the variables v , $s_{\phi,830}$, Δ_λ , G and the elements of Γ which are A_d , A_s and d

$u(x_i)$ = standard uncertainty of x_i

$u(x_i, x_j)$ is the covariance of x_i and x_j (assumed to be zero in this measurement)

The uncertainty of each variable is estimated and the value may be determined experimentally (Type A), such as the case with v from replicate measurements and Δ_λ and T from a spectrometric measurements. The uncertainty in the photodiode's spectral power responsivity $s_{\phi,\lambda}$ comes from the calibration [6] and the uncertainty in gain G is given by the manufacturer specification of the preamplifier used (Type B). The optical system throughput Γ is the arrangement of lenses, filters, baffles, apertures, that collects incoming light that give rise to the signal. Many factors affect throughput. This includes the filter transmittance, stray light, as well as dimensional measurements of aperture areas, solid angle and distances. Table 1 is a partial list of possible sources of uncertainty in measuring radiance from the tissue phantom using the photodiode. The effort to reduce uncertainties requires careful cataloguing of possible sources and refining the measurement through better instrumentation and procedures.

Evaluating the contribution of each variable to the combined uncertainty in the measurand is useful in prioritizing effort and resources to minimize the combined uncertainty. For instance, in Table 1, the major contributors to uncertainty in the radiance L_{830} are the voltage signal measurements which are dominated by random (Type A) uncertainties, the filter bandwidth and the filter transmittance. The filter bandwidth and transmittance uncertainties can be reduced by finer spectroscopic measurements and the voltage signal uncertainty can be reduced by replicate measurements.

Variable	Unit	Value	Standard Unc.	Type	Relative Sensitivity	Relative Unc	Total Rel Uncertainty	Rel Variance Fraction
x_i			$u(x_i)$		$c_{i,r}$	$(u(x_i)/x_i)$	$c_i^2 \cdot \left(\frac{u(x_i)}{x_i}\right)^2$	$\left(\frac{u(x_i)}{x_i}\right)^2 / \left(\frac{u_c(L_{830})}{L_{830}}\right)^2$
Signal v	V	0.1199	0.006	A,B	1	5.0E-2	2.5E-3	0.43
$s_{\phi,830}$	A W ⁻¹	0.4411	0.1%	B	1	1.0E-3	1.0E-6	0.00
$\Delta\lambda$	nm	9.3	4.0E-1	A	1	4.3E-2	1.9E-3	0.32
G	V A ⁻¹	10 ⁹	1%	B	1	1.0E-2	1.0E-4	0.02
d	m	0.577	2.1E-3	A	2	3.6E-3	5.3E-5	0.01
T		0.66	0.024	A	1	3.6E-2	1.3E-3	0.23
A_d	m ⁻²	1.1E-4	4.4E-7	A	1	4.1E-3	1.7E-5	0.00
A_s	m ⁻²	4.9E-5	4.4E-8	A	1	9.0E-4	8.0E-7	0.00
Combined Rel Uncertainty							7.7E-2	1.00
L_{830}	Wm ⁻² sr ⁻¹	2.8E-3						
$u_c(L_{830})$	Wm ⁻² sr ⁻¹	2.1E-4						

Table 1. The contributors to the uncertainty of a single radiance measurement from the tissue phantom fluorescence evaluated using the measurement Equation 2.

2.3 Measurements of Irradiance at Off Normal Observation Angles

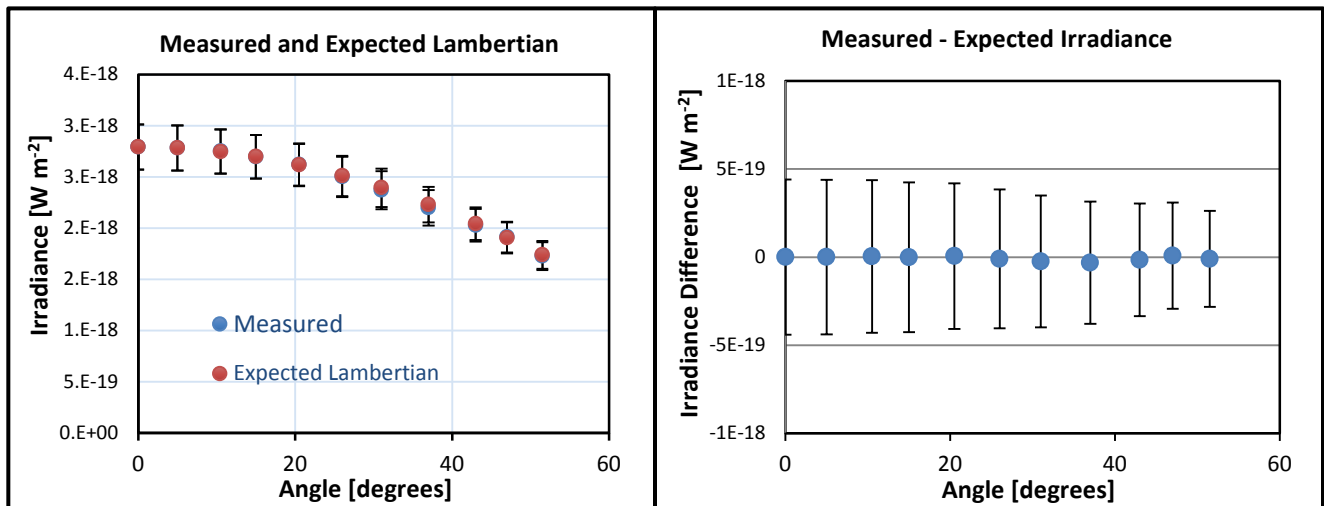


Figure 4. (Left) The measured and expected irradiances at off-normal angles if the source is Lambertian. (Right) The differences between the measured and expected irradiances are within the estimated uncertainties of 7% at $k=1$.

The tissue phantoms' emittance distribution over a range of angles from the normal position was measured using both the photodiode and the camera, similar to the radiance measurements in Section 2.1. The irradiance measured at 632 mm from the source is shown in Figure 4 (left) along with the expected irradiance for a Lambertian radiator at those

same angles computed from the irradiance measured at normal position (0°). The differences between the measured and computed irradiances are within the estimated uncertainties.

3. DISCUSSION AND FUTURE WORK

The measurement configuration used in this measurement is meant to mimic that of a clinical imager viewing the patient at a distance of about 600 mm and the excitation light incident at 45 degrees from the tissue phantom surface. We have shown in these few measurements that the tissue phantoms behave similarly to a lamp calibrator. Unlike a lamp calibrator with emission and over a wide spectral range, the tissue phantom is designed to have radiance output at the radiance level of the fluorophores emitting from inside the body and only at the desired spectral range. The choice of radiance as the radiometric quantity to ascribe to the tissue phantom enables the user to evaluate stray light issues with the collection geometry since radiance does not vary with distance. We have shown in Table 1 that the radiance measurement uncertainty is estimated to be at 7 % at a coverage of $k=1$. A similar procedure will be used to determine the uncertainty in irradiance of the excitation light incident on the surface to give the total uncertainty estimate for $F_{\lambda_{em},\lambda_{ex}}$, the calibration values for the tissue phantom for a range of excitation irradiances.

In order for the tissue phantoms to be useful as a reference material bearing radiometric units, its properties as a radiator need to be known. In this short experiment, we have verified that the tissue phantoms show evidence of being a Lambertian radiator; it does not show anomalous radiance at some angles as it would if the fluorescence emitted were somehow directional. This is not surprising given that the quantum dots are dispersed with highly scattering titanium dioxide. Calibration at a single position, typically at detection normal to the tissue phantom surface, is sufficient. If the tissue phantom is viewed at angles differing from surface normal, its radiance will be the same. Since the measurements were taken only at a single angle of incidence for the excitation light and a single viewing plane, this does not offer a complete picture of the hemispherical reflectance and fluorescence angular emission. Measurements using the NIST Robotic Optical Scatter Instrument (ROSI) [7], a goniometer where any combination of angles of incidence and viewing is possible, are planned; this will require some modifications to the instrument for fluorescence detection.

The tissue phantoms consisting of quantum dots dispersed with titanium dioxide in a polyurethane matrix offers a convenient way by which an optical calibration scale can be transferred from a reference detector (calibrated photodiode) to an imager. The calibrated tissue phantom can be presented to different imagers and each imager's response in arbitrary units can be converted to SI-traceable radiometric units.

ACKNOWLEDGEMENT

This material is based upon work supported by the NIST Summer Undergraduate Research Fellowship (SURF) Program. The authors also thank John Woodward for the filter transmittance measurements in the NIST SIRCUS facility.

REFERENCES

-
- [1] Litorja, M., Urbas, A. and Zong, Y. "Radiometric calibration methods to consider in quantitative clinical fluorescence imaging measurements," Proc. SPIE 9311, 931114 (2015).
 - [2] Zhu, B., Rasmussen, J. C. and Sevick-Muraca, E. M. "A matter of collection and detection for intraoperative and noninvasive near-infrared fluorescence molecular imaging: To see or not to see?" Med. Physics, 41(2), 022105(2014).
 - [3] Zhu, B., Rasmussen, J., Litorja, M., Sevick-Muraca, E.M. "Determining the Performance of Fluorescence Molecular Imaging Devices using Traceable Working Standards with SI Units of Radiance," IEEE Transactions on Medical Imaging, 35(3), 802-811(2016).
 - [4] McCluney, R., [Introduction to Radiometry and Photometry], Artech House, Boston and London, 13-15 (1994).
 - [5] Taylor, B.N. and Kuyatt, C.E. "Guidelines for Evaluating and Expressing the Uncertainty of NIST Measurement Results," NIST TN 1297 (1994). Available at <http://www.physics.nist.gov/Pubs>
 - [6] Larason, T.C., and Houston, J.M. "NIST Measurement Services: Spectroradiometric Detector Measurements: Ultraviolet, Visible and Near-Infrared Detectors for Spectral Power," NIST Special Publications 250-41 (2008).
 - [7] Patrick, H.J., Zarobila, C.J. and Germer, T.A., "The NIST Robotic Optical Scatter Instrument (ROSI) and its Application to BRDF Measurements of Diffuse Reflectance Standards for Remote Sensing," Proc. SPIE 8866, 886615-1-12 (2013).